Kinetic Study of the Shape Change of Human Erythrocyte Induced by Sodium Alkyl Sulfates

Katsuaki Inoue, Takako Sekido, and Takayuki Sano*,#

Department of Materials Science, Faculty of Science, Hiroshima University, Kagamiyama, Higashihiroshima, Hiroshima 739

(Received May 14, 1997)

In order to clarify the mechanism of the shape change of human erythrocytes induced by anionic surfactants, kinetic experiments were performed using the stopped-flow technique and the conventional spectroscopic method. In the time range from 0.1 s to a few dozen minutes, four kinetic processes were observed. In the dead time of the stopped-flow apparatus (within 10 milli seconds), a decrease in the intensity of the transmitting light was observed. Based on an analysis of the dependence of the relaxation time of each process on the surfactant concentration for various reaction schemes, we propose a most plausible reaction model that includes four kinds of binding processes of the surfactant and three intramolecular processes. In the present paper, based on this model, we discuss the detailed mechanism of the shape change of the erythrocytes.

The erythrocyte membrane comprises a phospholipid bilayer, membrane proteins, and skeletal proteins that support the lipid bilayer from the cytoplasmic side.[1,2] Hemoglobin and other soluble components are contained in the erythrocyte. The biconcave-disk shape of the erythrocyte is maintained through the interactions of these integrated components and the osmotic balance between the inside and the outside of the erythrocyte. Its shape can be made to vary through various operations, such as the addition of electrolytes or amphiphiles. Generally, electrolytes and anionic amphiphiles induce a shape change in the echinocyte (sphere with small spicules), and cationic amphiphiles induce it in the stomatocyte (cup form).[3] So far, we have studied the mechanism of shape change in an echinocyte induced by electrolytes statically and kinetically, and have clarified that the shape change induced by electrolytes progresses via two steps: (1) a rapid (within 1 s) shape-changing step from the normal biconcave disk to a flat disk due to water efflux caused by a difference in the osmotic pressure between the inside and the outside of the erythrocyte; (2) a slow shape-changing step from a flat disk to an echinocyte caused by a conformational change of the skeletal proteins and changes in the soluble components of the cytoplasm.[4]

Meanwhile, for the mechanism of a shape change induced by amphiphiles, the "bilayer couple hypothesis" proposed by Sheets and Singer has been generally accepted.[5] In this hypothesis they have stated that the anionic amphiphiles stay in the outer layer of the lipidbilayer because of an electric repulsion between the negative charges of the polar head group and the acidic phospholipids, which have negative charges (under physiological conditions), and are localize in the inner layer of the lipid bilayer. They thus cause the outer layer to expand more than the inner layer, so that the erythrocyte transforms into an echinocyte. At the same time, the cationic amphiphiles intercalate into the inner layer preferentially, because of an electrostatic attraction between their polar head group and acidic phospholipids, and then induce shape changes in the stomatocyte. Clarifying the mechanism of such shape changes is very significant because it would lead to not only a clarification of the correlation between the membrane structure and its functions but also would provide a comprehensive understanding of the action mechanism of drugs. Although several investigations have been carried out,[6—10] ambiguity concerning the mechanism of the shape change induced by amphiphiles remains. We chose sodium alkyl sulfate from a typical anionic amphiphile as an echinocyte inducer, because of its simple molecular structure, and because we had already performed binding experiments with it on human erythrocytes using surfactant ion selective electrodes, and differential scanning calorimetry (DSC) measurements to elucidate the binding manner and the binding site of surfactants on the erythrocyte membrane.[11] In the binding experiments with surfactant ion selective electrodes, it was found that all of the surfactants studied bound to the erythrocyte in two steps in the concentration range where a shape change occurred. Analyzing the binding ithoserms, it was clarified that the first binding is stronger than the second binding, and that the hydrophobic interaction between the alkyl chain of the surfactants and the erythrocyte is a main driving force for each binding. Further, utilizing DSC measurements for the erythrocyte ghost, the binding site of the surfactants on the erythrocyte membrane can be determined from the peak shift of the DSC spectrum. Brandts el al. had already found that the DSC of the erythrocyte ghost has five peaks — A ($T_m = 50°C$), B_1 ($T_m = 55°C$), B_2 ($T_m = 62°C$), C

Present address: Department of Physics, Oita Medical University, Hasama-machi, Oita 879-55, Japan.

($T_m = 67°C$) and D ($T_m = 77°C$) — and that these transitions could be attributed to the thermal transition of spectrin (A), the lipid boundary of band 4.1 and band 4.2 (B_1), the lipid boundary of band 3 (B_2), the lipid bilayer (C), and other proteins (D), respectively.[15,16,19] We utilized their method for the erythrocyte–sodium alkyl sulfate system and observed following things: 1) At the concentration range where only the first binding of the surfactant was observed, the peak temperature of B_2 shifted down by 3 °C, while the other peaks did not shift. 2) When the second binding was observed, the peak temperature of C also shifted down by 3 °C, accompanied by a shifting down of the peak temperature of B_2. From these experiments, it was shown that sodium alkyl sulfates bound in two steps, and that their binding sites were the boundary lipid region of band 3, one of the membrane proteins of the erythrocyte, and the lipid region of the membrane. In order to elucidate such a mechanism, however, kinetic experiments are indispensable and provide very useful information. Thus, in the present study, in order to understand in more detail the mechanism of the shape change, we performed kinetic experiments using a stopped-flow apparatus and the conventional spectroscopic method. Combining the results from both the static and kinetic experiments, we have proposed a model of the mechanism for the shape change of the human erythrocyte induced by sodium alkyl sulfates.

Materials and Methods

Reagents. The reagents used in the present study were of guaranteed grade and were used without further purification.

Surfactants. In the present study, sodium alkyl sulfates ($C_nH_{2n+1}OSO_3Na$), anionic surfactants, were used as an echinocyte inducer. Among these surfactants, we chose sodium hexyl sulfate (C_6), sodium octyl sulfate (C_8), sodium decyl sulfate (C_{10}), and sodium dodecyl sulfate (C_{12}). C_{12} was for biochemistry, and was purchased from Wako Pure Chemicals Co. The other three surfactants were synthesized according to Dreger el al.[12] and recrystallized two times from ethanol. The purity of the synthesized surfactants was estimated at 99.5% by elementary analysis and cmc measurements.

Preparation of Erythrocytes. Blood was drawn from the healthy adults by vein puncture into heparinized tubes. Erythrocytes were separated from heparinized blood by a 900 *g* centrifugation, and washed five times with a buffer containing 140 mM NaCl, 20 mM Tris-HCl (1 M = 1 mol dm^{-3}) at pH 7.4 (isoTBS). The erythrocytes were prepared within a few hours after drawing blood and were used with dilution by isoTBS to the appropriate concentration. The prepared erythrocytes were utilized for experiments within 48 h, and kept at 4 °C until just before use, to prevent spontaneous transformation into echinocyte shapes, even in isoTBS.

Kinetic Experiments. Kinetic experiments were undertaken mainly using a stopped-flow apparatus (RA-401, Unisoku Co., Ltd.) with optical detection, such as the transmittance and scattering intensity of light. In the case of transmittance detection, the wavelength of detection was chosen to be $\lambda = 485$ nm, and in the case of scattering light detection, $\lambda = 365$ nm was applied because of the small absorption of hemoglobin and the large amplitude of the reaction. The experiments were carried out at 37±1°C. The erythrocyte concentration was kept at 0.15% hematocrit (2.4×10^7 cells mL^{-1}). Prior to the kinetic experiments, observations of the erythrocyte shape and the hemolysis experiments were carried out using the same procedures as previously reported.[11] Generally, in an extra low-concentration range of the surfactants, a shape change in erythrocytes does not occur; that is, a shape change is induced only above the critical concentration of the surfactants. Moreover, in a high-concentration range, surfactants induce the hemolysis of erythrocytes. Since the object of the present work was to investigate only the shape change, we chose the optimal concentration range for the kinetic experiments from microscopic observations and hemolysis experiments. Only then was the concentration range of each surfactant decided: for C_6, 4—20 mM, for C_8, 1—7 mM, for C_{10}, 50—400 μM, and for C_{12}, 5—40 μM. The kinetic experiments were carried out at several points within each concentration range. These concentration ranges were significantly lower than the cmc of each surfactant, suggesting that only the surfactant monomers participate in the shape change of the erythrocyte.

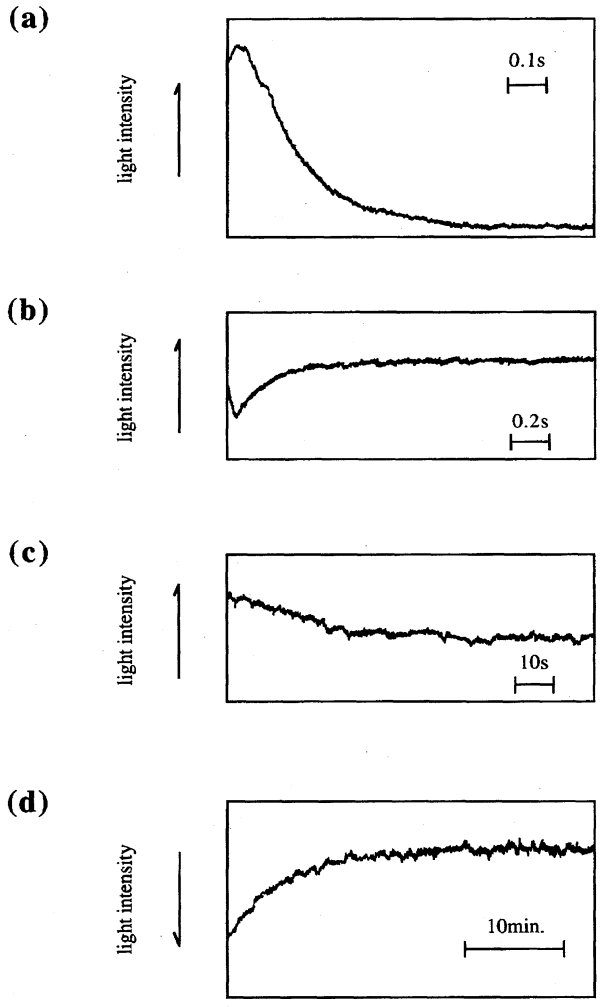

Fig. 1. Typical reaction curves observed (a) in process 1 (P_1) with transmitting light detection, (b) in process 2 (P_2) with scattering light detection, (c) in process 3 (P_3) with scattering light detection and (d) in process 4 (P_4) with transmitting light detection in erythrocyte–C_{10} system. The concentration of C_{10} was (a) 50 μM, (b) 300 μM, (c) 250 μM, and (d) 100 μM. The detection wavelength is $\lambda = 485$ for the transmitting light and $\lambda = 365$ for the scattering light.

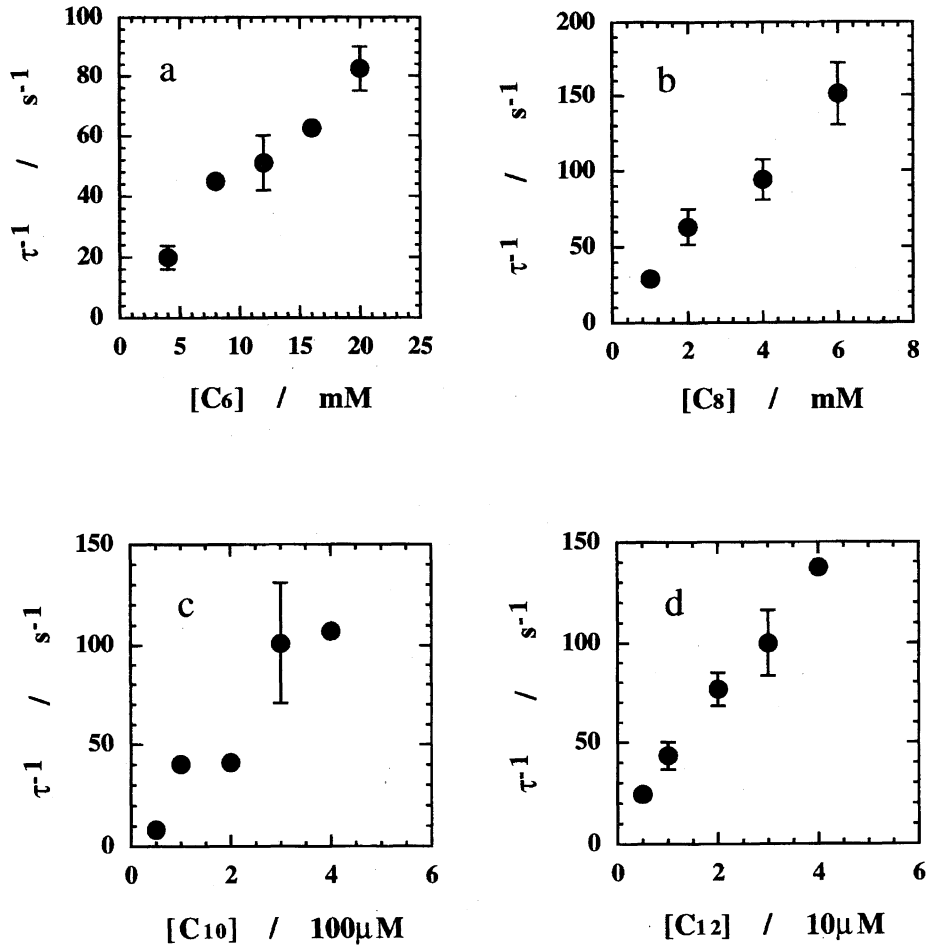

Fig. 2. The concentration dependence of τ^{-1} for process 1 (P_1) (a) for C_6, (b) for C_8, (c) for C_{10}, and (d) for C_{12}.

Table 1. Equilibrium Constants of Each Process

	K_0 / M^{-1}	K_1	K_2 / M^{-1}	K_3	K_3^* / M^{-1}	K_4	K_4^* / M^{-1}
C_6	0.5	7.99×10^2 (0.5)	7.22 (2.0)	2.63×10^{-3} (0.7)	7.5×10^4	3.83×10^{-3} (0.9)	5.0×10^4
C_8	0.75	3.75×10^3 (0.8)	68.6 (16)	1.54×10^{-3} (0.3)	2.5×10^5	4.32×10^{-3} (0.6)	2.5×10^5
C_{10}	1.0	1.08×10^5 (0.4)	1.93×10^3 (0.5)	1.49×10^{-3} (0.4)	1.0×10^6	2.21×10^{-2} (0.4)	7.5×10^5
C_{12}	1.5	3.17×10^6 (1.5)					

The numerals in the parenthesis on the table are standard deviations.

Results

Before the kinetic experiments, optical-microscope observations were performed. As previously reported,[11] first, the erythrocyte became a sphere with short, small spicules (sphero-echinocyte defined by Bessis[13]), at latest, within 10 s after the addition of the surfactants; then, those spicules became larger (echinocyte III[13]) within the next 20 min. These shape-change steps were observed with good reproducibility, and were the same for all surfactants. It, furthermore, corresponded to those observed by Isomaa et al.[6] Figs. 1a, 1b, 1c, and 1d show typical reaction curves observed by optical detection for the shape changes induced by sodium alkyl sulfates. In the time range from 0.1 s to a few dozen minutes, four kinetic processes were observed. In the dead time of the stopped-flow apparatus (within 10 milli seconds), although a decrease in the intensity of the transmitting light was observed, no reaction curve was obtained. We defined these processes as process 0 (P_0), process 1 (P_1), process 2 (P_2), process 3 (P_3), and process 4 (P_4), in the order of their rate. P_1 and P_4 were observed by transmitting light detection and P_2 and P_3 by scattering light detection. P_0, P_1, and P_4 were

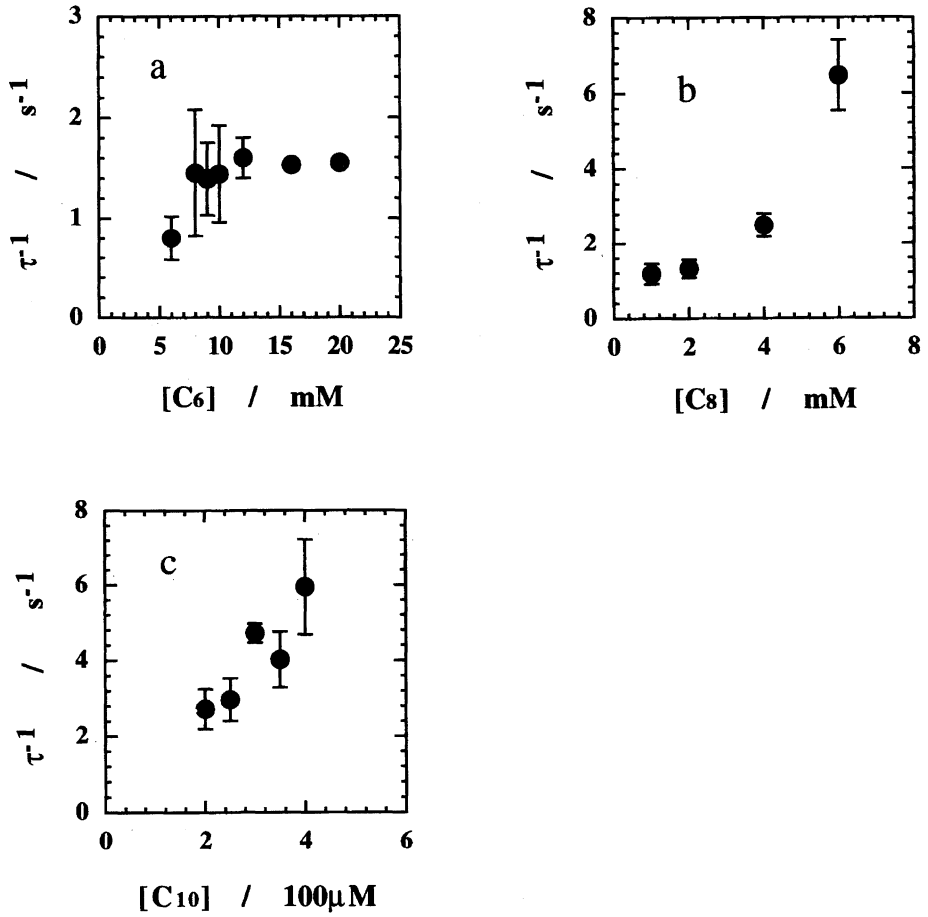

Fig. 3. The concentration dependence of τ^{-1} for process 2 (P_2) (a) for C_6, (b) for C_8, and (c) for C_{10}.

Table 2. Rate Constants of Each Process

	k_1 / s^{-1}	k_{-1} / s^{-1}	k_2 / $M^{-1}\,s^{-1}$	k_{-2} / s^{-1}	k_3 / s^{-1}	k_{-3} / s^{-1}	k_4 / s^{-1}	k_{-4} / s^{-1}
C_6	7.23×10^3	9.05	10.7	1.38	1.05×10^{-1}	40.4	1.76×10^{-2}	4.59
	(0.3)	(0.2)	(0.8)	(0.2)	(0.3)	(0.5)	(0.3)	(0.4)
C_8	3.11×10^4	8.31	16.4	0.239	2.25×10^{-3}	14.6	4.22×10^{-2}	9.77
	(0.5)	(0.4)	(0.5)	(0.04)	(0.5)	(0.3)	(0.5)	(0.4)
C_{10}	2.81×10^4	0.261	3.42×10^3	1.77	2.43×10^{-2}	16.3	3.77×10^{-2}	1.71
	(0.4)	(0.2)	(0.5)	(0.2)	(0.6)	(0.4)	(0.3)	(0.2)
C_{12}	2.03×10^6	0.641						
	(0.5)	(0.1)						

The numerals in the parenthesis on the table are standard deviations.

observed in all systems. In the C_{12} system, P_2 and P_3 were observed only at 40 μM; at lower concentrations, reaction curves were not observed because of the small amplitude. In the other three systems, P_2 and P_3 were observed at all measured points. Figures 2, 3, 4, and 5 show the concentration dependence of the relaxation time (τ^{-1}) of each process for the four surfactants. As shown in Figs. 2 and 3, τ^{-1} of P_1 and P_2 was positively dependent on the surfactant concentration. On the contrary, as shown in Figs. 4 and 5, τ^{-1} of P_3 and P_4 was negatively dependent. The τ^{-1} of each process was not dependent on the erythrocyte concentration (data not shown). This implies that the concentration of the surfactants is sufficiently higher than that of the binding site on the erythrocyte under the present experimental conditions.

Upon analyzing these kinetic data, we examined many reaction schemes for a shape change. Among these, we propose the following reaction scheme as being the best model (Scheme 1). In this scheme, P_0, P_2, P_3^*, and P_4^* represent the binding processes of the surfactant on the erythrocyte. P_1, P_3, and P_4 represent the intramolecular processes of the complex between the surfactant and the erythrocyte. P_3^* equilibrates faster than P_3. P_4^* equilibrates faster than P_4. To interpret the negative dependence of τ^{-1} on the surfactant concentration, such as P_3 and P_4, more satisfactorily,

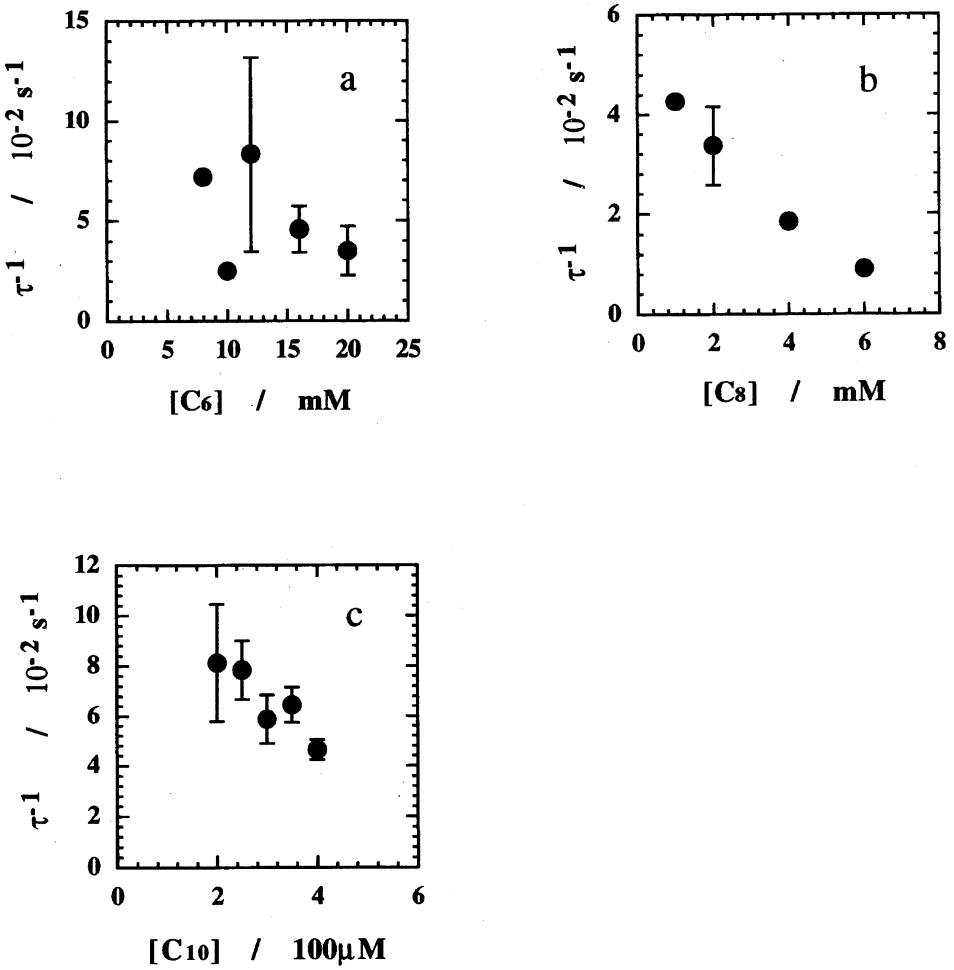

Fig. 4. The concentration dependence of τ^{-1} for process 3 (P_3) (a) for C_6, (b) for C_8, and (c) for C_{10}.

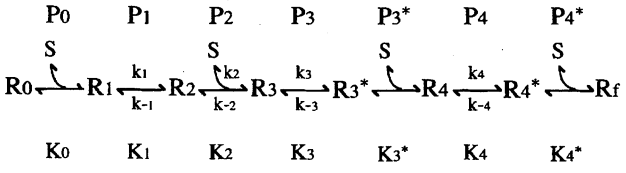

Scheme 1.

the intramolecular process coupled with the subsequent fast surfactant binding process was considered. Thus, P_3^* and P_4^* were introduced into the reaction scheme. R_i, in the scheme, denotes the binding site of the erythrocyte and S denotes the free surfactants. From the rate equations for each process, the following formulas of the relaxation time for each process were derived as the function of [S] and the equilibrium constants for each process with the condition that $[R_0]$ was much smaller than [S]. The derivation of these formulas is summarized in the Appendix.

For P_1,

$$\tau_1^{-1} = \frac{K_0[S]}{1+K_0[S]}k_1 + k_{-1}. \quad (1)$$

For P_2,

$$\tau_2^{-1} = \frac{K_0K_1[S]^2}{1+K_0[S]+K_0K_1[S]}k_2 + k_{-2}. \quad (2)$$

For P_3,

$$(1+K_3^*[S])\tau_3^{-1} = Bk_3 + k_{-3}, \quad (3)$$

with

$$B = \frac{(1+K_3^*[S])K_0K_1K_2[S]^2}{1+K_0[S]+K_0K_1[S]+K_0K_1K_2[S]^2}.$$

For P_4,

$$(1+K_4^*[S])\tau_4^{-1} = Dk_4 + k_{-4}, \quad (4)$$

with

$$D = \frac{(1+K_4^*[S])K_0K_1K_2K_3K_3^*[S]^3}{1+K_0[S]+K_0K_1[S]+K_0K_1K_2[S]^2+K_0K_1K_2K_3[S]^2+K_0K_1K_2K_3K_3^*[S]^3}.$$

[S] indicates the molar concentrations of the free surfactant. In analyzing P_1, assuming the value of K_0 in Eq. 1, the concentration term on the right-hand side in Eq. 1 was plotted against τ^{-1} and the rate constants k_1 and k_{-1}, obtained from the slope and the intercept. The equilibrium constant of P_1 (K_1) was calculated from $K_1=k_1/k_{-1}$. In analyzing P_2, the concentration term on the right-hand side in Eq. 2 was plotted against τ^{-1} and the rate constants k_2 and k_{-2}, obtained from the slope and the intercept. The equilibrium constant (K_2) was calculated from $K_2=k_2/k_{-2}$. As for analyzing P_3 and P_4, assuming values of K_3^* and K_4^*, the terms on the left-handed side in Eqs. 3 and 4 can be plotted against terms B and D, respectively. The rate constants k_3, k_{-3}, k_4, and k_{-4} could be obtained from the slope and the intercept of these plots. In

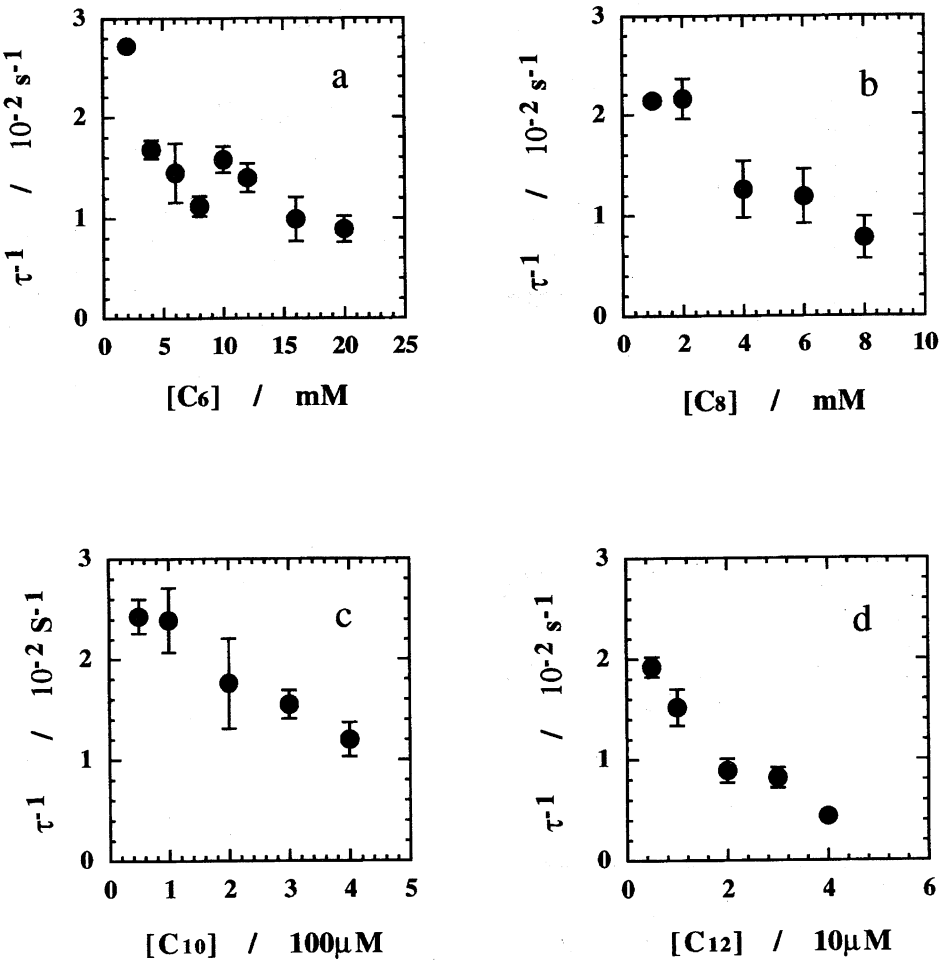

Fig. 5. The concentration dependence of τ^{-1} for process 4 (P_4) (a) for C_6, (b) for C_8, (c) for C_{10}, and (d) for C_{12}.

the same manner as the analysis of P_1 and P_2, the equilibrium constants (K_3 and K_4) were calculated from $K_3=k_3/k_{-3}$ and $K_4=k_4/k_{-4}$. Typical examples of these analyses are shown in Fig. 6. As can be seen in these figures, each process was analyzed satisfactorily based on the above formulas. In analyzing any other models (e.g. the scheme which includes only two binding processes or three binding process), all of the observed processes could not be analyzed satisfactorily. That is, in all such cases, especially in analyzing P_3 or P_4, the intercept of the analyzing plot became negative, and the kinetic parameter could never be determined (data not shown). It was thus concluded that this Scheme 1 is the best model for the shape change of the erythrocyte. The evaluated equilibrium constants are listed in Table 1. The evaluated rate constants are listed in Table 2. Figure 7 shows the dependence of the equilibrium constants on the alkyl chain length of the surfactants. As for K_0, it does not show as great a dependence on the hydrophobicity of the surfactant, and it seems that the stabilization of the complex by the binding of the surfactant is small because K_0 is not very large. The complex, however, can be stabilized to a greater degree by the following intramolecular process (P_1). Furthermore, from the dependence of K_1 on the alkyl chain length of the surfactant, it was found that the effect of stabilization becomes greater as the alkyl chain of the surfactant becomes longer. This is because the rate of the forward reaction increases and that of the backward reaction decrease as the alkyl chain becomes longer, as can be seen for k_1 and k_{-1} in Table 2. As for K_2, it becomes larger as the alkyl chain of the surfactant becomes longer. A similar tendency can be seen in the forward rate constants of this process (k_2, in Table 2), although the backward rate constants (k_{-2}) are almost constant. This suggests that in the binding process of P_2, the hydrophobic interaction between the alkyl chain of the surfactant and the erythrocyte membrane mainly contributes to the binding of the surfactant to the erythrocyte. As can be seen in Table 1 and Fig. 7, K_3 and K_4 are smaller than 1, which is due to the fact that k_{-3} and k_{-4} are larger than k_3 and k_4, respectively. However, K_3^* and K_4^* are very large. Thus, the shape change could progress through this reaction scheme. Moreover, K_3^* and K_4^* increase as the alkyl chain becomes longer (Fig. 7 and Table 1). This also suggests that the hydrophobic interaction between the alkyl chain and the erythrocyte membrane is the main driving force of the binding in these processes.

Discussion

In a previous study, we carried out statical experiments[11] using home-made surfactant ion selective electrodes and DSC measurements, which were first attempted by Brandts

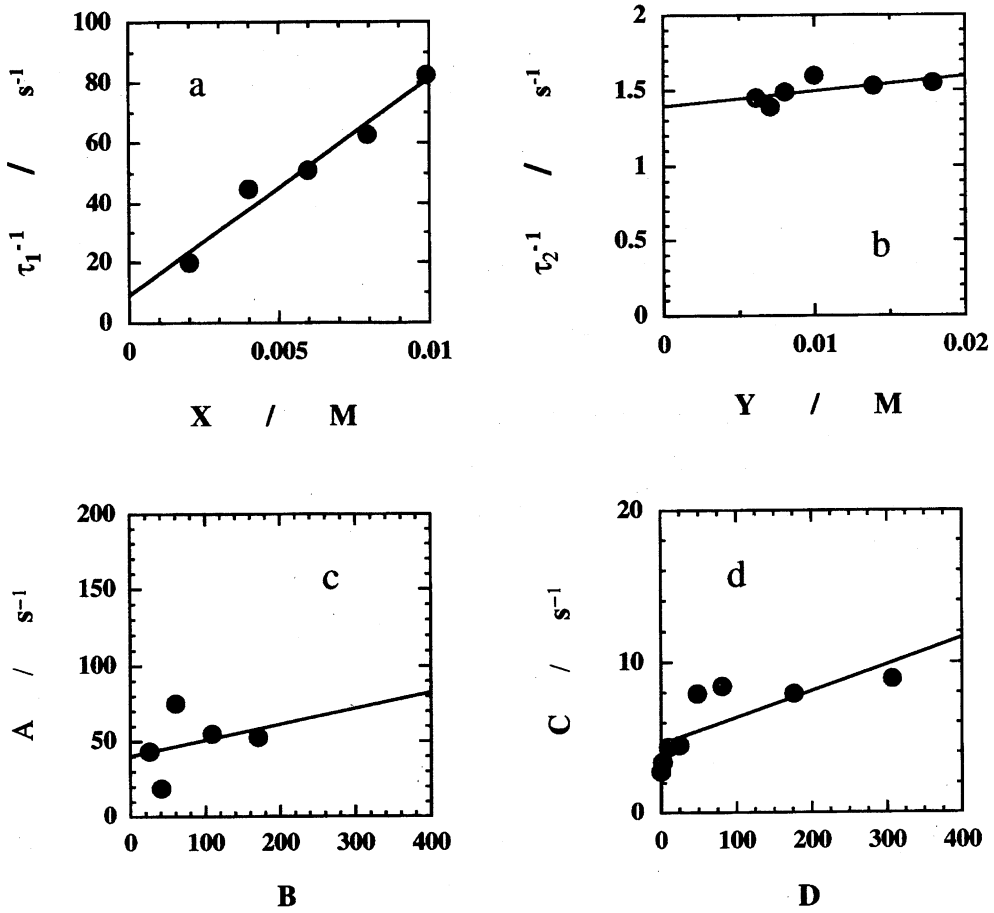

Fig. 6. Typical examples of the kinetic analysis (a) for process 1 (P_1) of C_6, (b) for process 2 (P_2) of C_6, (c) for process 3 (P_3) of C_6, and (d) for process 4 (P_4) of C_6. $X=\frac{K_0([R_0]+[S])}{1+K_0([R_0]+[S])}$, $Y=\frac{K_0K_1([R_0]+[S])([R_2]+[S])}{1+K_0([R_0]+[S])+K_0K_1([R_0]+[S])}$, $A=(1+K_3^*[S])\tau_3^{-1}$, $B=\frac{(1+K_3^*[S])K_0K_1K_2[S]^2}{1+K_0[S]+K_0K_1[S]+K_0K_1K_2[S]^2}$, $C=(1+K_4^*[S])\tau_4^{-1}$, and $D=\frac{(1+K_4^*[S])K_0K_1K_2K_3K_3^*[S]^3}{1+K_0[S]+K_0K_1[S]+K_0K_1K_2[S]^2+K_0K_1K_2K_3[S]^2+K_0K_1K_2K_3K_3^*[S]^3}$.

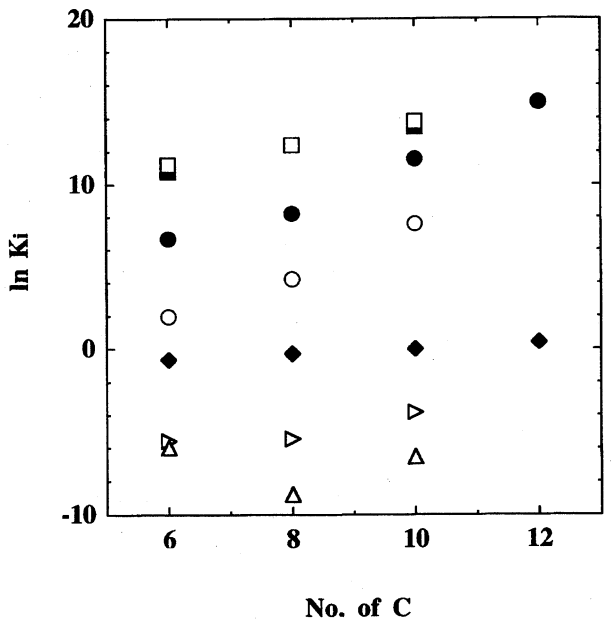

Fig. 7. Dependence of the equilibrium constants obtained in the kinetic experiments, K_0 : ◆, K_1 : ●, K_2 : ○, K_3 : △, K_3^* : □, K_4: ▷, and K_4^* : ■.

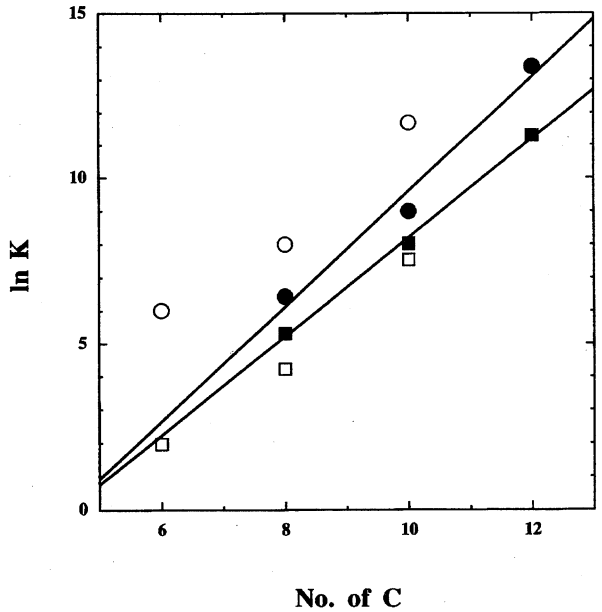

Fig. 8. Comparison of the equilibrium constants. K_I : ●, K_f^{ov} : ○, K_{II} : ■, and K_s^{ov} : □. The solid lines are the fitting lines of K_I and K_{II} which were calculated by the least squares method.

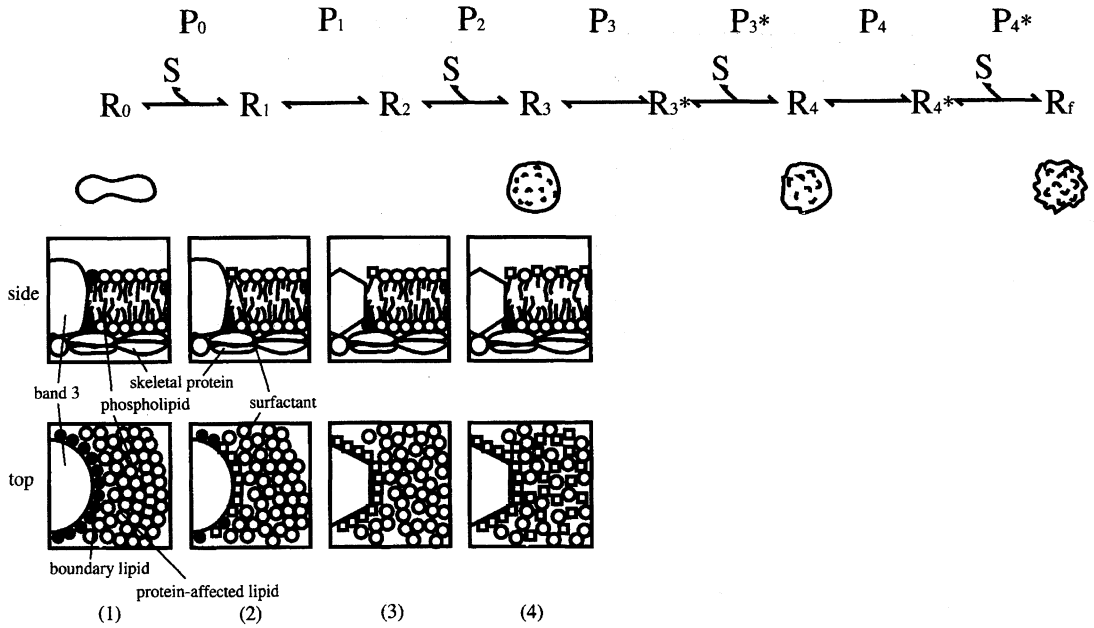

Fig. 9. Proposed scheme for the shape change of the erythrocyte and the illustrations of the shape of the erythrocyte and the erythrocyte membrane at each process. ○: the phospholipid molecules, ●: the boundary lipids and □: the surfactant molecules. (1) The normal erythrocyte. (2) After the first binding process. The surfactants exchange with the boundary lipids of band 3 and bind to band 3. (3) After the intracellular process in which the second binding sites are formed. In this process, the conformational change of band 3 occurs. (4) After the process of another binding of the surfactants.

et al.[14—20] From the binding experiments and DSC measurements, the following clarifications had been achieved: (1) The surfactants bind to the erythrocyte in two steps. In both steps, the equilibrium constants became larger as the alkyl chain became longer. (2) The first binding site is the boundary lipid region of band 3, one of the membrane proteins of the erythrocyte, and the second binding site is the phospholipid layer of the erythrocyte membrane. (3) The first binding of the surfactant leads to a conformational change of band 3, and, subsequently, to a structural change of the lipid region around band 3. The second binding sites are created on the lipid region. In order to interpret the present kinetic data satisfactorily, we examined many reaction schemes. Among those, Scheme 1 was determined to be the most plausible model of the shape change, because, as can be seen in Fig. 6, each process could be analyzed satisfactorily to obtain the kinetic parameters. This scheme consisted of seven processes, including the surfactant-binding process, within a few milli seconds after adding the surfactants (P_0): the intramolecular process from 0.1 s to within 1 s (P_1), the second surfactant-binding process in the time range of a few seconds (P_2), and two slow intramolecular processes coupled with the fast surfactant binding processes over the time range from a few seconds to a few minutes (P_3 and P_3^*, P_4 and P_4^*). From the present kinetic experiments, four binding processes of the surfactant were thought to exist in the whole shape-change mechanism, although two surfactant binding steps were observed in the static experiments.[11] In order to confirm the relation between the binding processes observed in the kinetic experiments and those in the static experiments, we compared the equilibrium constants from the kinetic experiments with those from the static experiments. The comparison is shown in Fig. 8. In this figure, K_I and K_{II} represent the equilibrium constants of the first binding and the second binding observed in the binding experiments, respectively. As can be seen in this figure, it was found that K_I corresponds to K_f^{ov}, which was the overall equilibrium constant included only the fastest binding process (P_0), within one order. K_{II} corresponded to K_s^{ov}, which was the overall equilibrium constant including three other binding processes (P_2, P_3^*, and P_4^*) within one order. It was thought that the binding constant and the binding site of these three bindings were the same because K_s^{ov} did not depend on the surfactant concentration. This implies that the fastest binding process (P_0) corresponded to the first binding in the binding isotherms, which was observed in the static experiments, and that the latter three binding processes (P_2, P_3^*, and P_4^*) were included in the second binding in the binding isotherms. From these facts, it was concluded that Scheme 1 satisfies not only the results from the kinetic experiments but also those from the static ones. Based on these findings, we considered that P_0 was the first surfactant binding process in the boundary lipid region of band 3, that P_1 was the process of structural change in the lipid region around band 3 caused by the conformational change of band 3, and that P_2, P_3^*, and P_4^* were the other surfactant binding processes at the new binding site on the lipid layer created by a structural change of the lipid region around band 3. Furthermore, a comparison with the results of optical microscope observations showed that the time range from P_2 to P_4^* corresponded to that of the enlarging process of the spicules on the surface of the erythrocyte. We determined that the processes from P_2 to P_4^* were the processes of spicule enlargement on the erythrocyte surface caused by the binding of the surfactants to the

lipid layer of the erythrocyte membrane. Thus, the following changes are thought to occur on the erythrocyte membrane (summarized schematically in Fig. 9): (1) The surfactants bind to the lipid boundary of band 3 by exchanging with boundary lipid molecules (P_0). (2) Accompanied by a conformational change of band 3 caused by the binding of the surfactant, the structure of the protein-affected lipid region changes, and, then, the protein-affected lipid region turns to the second binding sites (P_1). (3) Subsequently, surfactants begin to bind to this new binding site (P_2). Then, because of a structural change of the membrane and another binding of the surfactant, the spicules on the surface get larger (P_3, P_3^*, P_4, and P_4^*). As can be seen in Table 1 and Fig. 7, K_0 is about 1 for each surfactant, and becomes slightly larger as the alkyl chain length increases. This implies that, being different from other three binding processes, P_0 is a diffusion controlled process, although the hydrophobic interaction between the alkyl chain and the erythrocyte also participates in the binding. Additionally because P_0 is thought to be the diffusion controlled process, the first binding process might be too fast to observed with the stopped-flow technique. In P_2, P_3^*, and P_4^*, the hydrophobic interaction is thought to be the main driving force of the binding because the equilibrium constants of each process become larger as the alkyl chain length becomes longer. This is consistent with a model which considers that the second binding site is the lipid layer of the membrane. In the present study, it was found that τ^{-1} of P_3 and P_4 were negatively dependent on the surfactant concentration. Such a process was also observed in the erythrocyte–electrolyte systems studied in our laboratory previously.[4] In those studies, it was clarified that such a negative dependence of the τ^{-1} was observed in a slow intramolecular process, which is the shape-changing step from a flat disk to an echinocyte, and that this intramolecular process was caused by changes in the soluble components of the cytoplasm from experiments using erythrocyte ghosts and the Triton® shell, which was complex of the skeletal proteins of the erythrocyte extracted by Triton X®. Sodium alkyl sulfates, which bound to the erythrocyte membrane, are thought to remain in the outer layer of the lipid bilayer of the erythrocyte membrane because the inner layer, in which the negatively charged phospholipids exist, charges negatively.[21,22] Thus, they are thought to neither penetrate into the cytoplasm nor to affect the soluble components in the cytoplasm. However, considering the fact that band 3 is one of the anion channels of the erythrocyte, a structural change in band 3 may lead to a change in the ionic strength of the cytoplasm of the erythrocyte. It is possible that the change of the soluble components in the cytoplasm might affect the slow intramolecular processes. However, it was not possible to clarify the reason why two slow intramolecular processes exist in the erythrocyte–surfactant system, although only one process was observed in the erythrocyte–electrolyte system. This may be clarified through experiments using erythrocyte ghosts or the Triton® shell. Kinetic experiments of the shape change with optical detection were also attempted by Fujii et al. on the erythrocyte–amphiphiles system.[10] In their experiments, only one process was observed by means of the stopped-flow apparatus with scattering light detection. However, in the present study from kinetic experiments with two kinds of detection, such as transmittance and scattering light detection, it was found that at least five processes could be observed spectroscopically. It is clear that changes in the transmittance and scattering light reflect the shape change of the erythrocyte, but involve different information, such as the size of the erythrocyte or the surface structure of the erythrocyte. We, however, could not understand what kind of change on the erythrocyte shape the optical change of each process suggests, and what process Fujii et al. observed in the other amphiphile systems.[10] We next plan to carry out more precise time-resolved observations of the shape change with the newly developed stooped-flow microscope. The use of this apparatus will provide more detailed information about the relationship between the spectroscopically observed reaction curves and the actual shape of the erythrocyte in the near future. Through the present study we have shown that shape change occurs through complicated pathways, strongly suggesting that not only the phospholipid bilayer but also the membrane protein, especially band 3 and other components, play important roles in the mechanism of the shape change of the erythrocyte.

Appendix

The rate equation of each process are given as follows based on each scheme and the formulas of the relaxation time (Eqs. 1, 2, 3, and 4) are derived from each rate equation with the analytical procedures of the relaxation method under the following conditions.

For P_1, (Scheme 2):

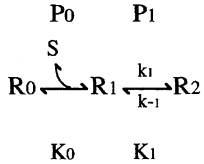

Scheme 2.

$$\frac{d[R_2]}{dt} = k_1[R_1] - k_{-1}[R_2],$$

with

$$\Delta[R_0] + \Delta[R_1] + \Delta[R_2] = 0.$$

P_0 equilibrates faster than P_1, so

$$K_0 = \frac{[R_1]}{[R_0][S]}$$

could be applied.

For P_2, (Scheme 3):

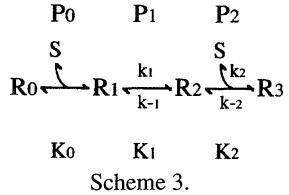

Scheme 3.

$$\frac{d[R_3]}{dt} = k_2[R_2][S] - k_{-2}[R_3],$$

with

$$\Delta[R_0] + \Delta[R_1] + \Delta[R_2] + \Delta[R_3] = 0.$$

P_0 and P_1 equilibrate faster than P_2, so

$$K_0 = \frac{[R_1]}{[R_0][S]}, \quad K_1 = \frac{[R_2]}{[R_1]}$$

could be applied.
For P_3, (Scheme 4):

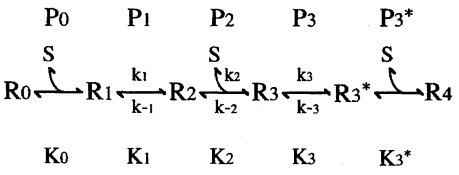

Scheme 4.

$$\frac{d([R_3^*] + [R_4])}{dt} = k_3[R_3] - k_{-3}[R_3^*],$$

with

$$\Delta[R_0] + \Delta[R_1] + \Delta[R_2] + \Delta[R_3] + \Delta[R_3^*] = 0.$$

P_0, P_1, P_2, and P_3^* equilibrate faster than P_3, so

$$K_0 = \frac{[R_1]}{[R_0][S]}, \quad K_1 = \frac{[R_2]}{[R_1]}, \quad K_2 = \frac{[R_3]}{[R_2][S]}, \quad K_3^* = \frac{[R_4]}{[R_3^*][S]}$$

could be applied.
For P_4, (Scheme 5):

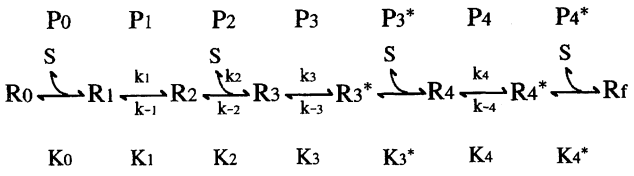

Scheme 5.

$$\frac{d([R_4^*] + [R_f])}{dt} = k_4[R_4] - k_{-4}[R_4^*],$$

with

$$\Delta[R_0] + \Delta[R_1] + \Delta[R_2] + \Delta[R_3] + \Delta[R_3^*] + \Delta[R_4] + \Delta[R_4^*] + \Delta[R_f] = 0.$$

P_0, P_1, P_2, P_3, and P_3^* equilibrate faster than P_4, so

$$K_0 = \frac{[R_1]}{[R_0][S]}, \quad K_1 = \frac{[R_2]}{[R_1]}, \quad K_2 = \frac{[R_3]}{[R_2][S]}, \quad K_3 = \frac{[R_3^*]}{[R_3]},$$
$$K_3^* = \frac{[R_4]}{[R_3^*][S]}, \quad K_4^* = \frac{[R_f]}{[R_4^*][S]}$$

could be applied.

References

1) V. Bennett, *Ann. Rev. Biochem.*, **54**, 273 (1985).
2) A. Elgsaeter, B. T. Stokke, A. Mokkelsen, and D. Branton, *Science*, **234**, 1217 (1986).
3) B. Deuticke, *Biochim. Biophys. Acta*, **163**, 494 (1968).
4) H. Ouchi, I. Hayashi, T. Nakata, K. Hadani, K. Inoue, and T. Sano, unpublished data.
5) M. P. Sheets and S. J. Singer, *Proc. Natl. Acad. Sci. U.S.A.*, **71**, 4457 (1974).
6) B. Isomaa, H. Hägerstrand, and G. Paatero, *Biochim. Biophys. Acta*, **899**, 93 (1987).
7) H. Hägerstrand and B. Isomaa, *Biochim. Biophys. Acta*, **982**, 179 (1989).
8) H. Hägerstrand and B. Isomaa, *Biochim. Biophys. Acta*, **1109**, 117 (1992).
9) H. Hägerstrand and B. Isomaa, *Biochim. Biophys. Acta*, **1190**, 409 (1994).
10) T. Fujii, A. Tamura, T. Tanaka, H. Nagasawa-Fujimori, and K. Hiromi, *Biochem. Int.*, **8**, 83 (1984).
11) K. Inoue, T. Sekido, and T. Sano, *Langmuir*, **12**, 4644 (1996).
12) E. E. Dreger, G. I. Keim, G. D. Miles, L. Shedlovsky, and J. Ross, *Ind. Eng. Chem.*, **36**, 610 (1944).
13) M. Bessis, in "Red Cell Shape; Physiology, Pathology, Ultrastructure," ed by M. Bessis, R. I. Weed, and P. F. Leblond, Springer-Verlag, Heidelberg (1973), p. 1.
14) W. M. Jackson, J. Kostyla, J. H. Nordin, and J. F. Brandts, *Biochemistry*, **12**, 3662 (1973).
15) J. F. Brandts, K. Lysko, A. T. Schwartz, L. Erickson, R. B. Carlson, J. Vincentelli, and R. D. Taverna, "Colloques Internationaux du C. N. R. S.," 1976, p. 246, L'eau et les systemes biologiques, p. 169.
16) J. F. Brandts, L. Erickson, K. Lysko, A. Schwartz, and R. D. Taverna, *Biochemistry*, **16**, 3450 (1977).
17) K. S. Krishnan and J. F. Brandts, *Mol. Pharmacol.*, **16**, 181 (1979).
18) P. S. Low and J. F. Brandts, *Arch. Biochem. Biophys.*, **190**, 640 (1978).
19) J. F. Brandts, R. D. Taverna, E. Sadasivan, and K. Lysko, *Biochim. Biophys. Acta*, **512**, 566 (1978).
20) J. W. Snow, J. F. Brandts, and P. S. Low, *Biochim. Biophys. Acta*, **512**, 579 (1978).
21) B. R. Lentz, K. W. Clubb, D. R. Alford, M. Hochli, and G. Meissner, *Biochemistry*, **24**, 433 (1985).
22) R. B. Gennis, "Biomembranes," Springer-Verlag, Tokyo (1990), p. 161.